HHS Public Access

Author manuscript

Brain Imaging Behav. Author manuscript; available in PMC 2019 April 01.

Published in final edited form as:

Brain Imaging Behav. 2018 April ; 12(2): 532–546. doi:10.1007/s11682-017-9721-z.

Positron emission tomography assessment of cerebral glucose metabolic rates in autism spectrum disorder and schizophrenia

Serge A. Mitelman[1,2,*], **Marie-Cecile Bralet**[3,4,5], **M. Mehmet Haznedar**[1,6], **Eric Hollander**[7], **Lina Shihabuddin**[1], **Erin A. Hazlett**[1,8], and **Monte S. Buchsbaum**[9]

[1]Departments of Psychiatry and Neuroscience, Icahn School of Medicine at Mount Sinai, One Gustave L. Levy Place, New York, New York 10029, USA

[2]Department of Psychiatry, Division of Child and Adolescent Psychiatry, Elmhurst Hospital Center, 79-01 Broadway, Elmhurst, New York 11373, USA

[3]Crisalid Unit (FJ5), CHI Clermont de l'Oise, 2 rue des Finets, 60607, Clermont, France

[4]Inserm Unit U669, Maison de Solenn, Universities Paris 5–11, 75014, Paris, France

[5]GDR 3557 Recherche Psychiatrie, Paris, France

[6]Outpatient Psychiatry Care Center, James J. Peters VA Medical Center, Bronx, New York 10468, USA

[7]Autism and Obsessive-Compulsive Spectrum Program, Anxiety and Depression Program, Department of Psychiatry and Behavioral Science, Albert Einstein College of Medicine and Montefiore Medical Center, Bronx, New York 10467, USA

[8]Research and Development and VISN 2 Mental Illness Research, Education, and Clinical Center, James J. Peters VA Medical Center, Bronx, New York 10468, USA

[9]Departments of Psychiatry and Radiology, University of California, San Diego School of Medicine, NeuroPET Center, 11388 Sorrento Valley Road, Suite #100, San Diego 92121, USA

Abstract

Several models have been proposed to account for observed overlaps in clinical features and genetic predisposition between schizophrenia and autism spectrum disorder. This study assessed

[*]Corresponding author: Serge A. Mitelman. serge.mitelman@mssm.edu, Address: Department of Psychiatry, Division of Child and Adolescent Psychiatry, Elmhurst Hospital Center, 79-01 Broadway, Elmhurst, New York, 11373, USA. Tel. (718)334-2646.

Compliance and ethical standards

Author Serge A. Mitelman declares that he has no conflict of interest to report.
Author Marie-Cecile Bralet declares that she has no conflict of interest to report.
Author M. Mehmet Haznedar declares that he has no conflict of interest to report.
Author Eric Hollander has received consultation fees from Transceit, Neuropharm, and Nastech.
Author Lina Shihabuddin declares that she has no conflict of interest to report.
Author Erin A. Hazlett declares that she has no conflict of interest to report.
Author Monte S. Buchsbaum declares that he has no conflict of interest to report.
All procedures performed in this study were in accordance with the ethical standards of the Mount Sinai institutional research committee, as well as with the 1964 Helsinki declaration and its later amendments. The project was approved by the institutional review board of The Icahn School of Medicine at Mount Sinai. Informed consent was obtained from all individual participants in the study.

similarities and differences in topological patterns and vectors of glucose metabolism in both disorders in reference to these models.

Co-registered ^{18}F-FDG PET and MRI scans were obtained in 41 schizophrenia, 25 ASD, and 55 healthy control subjects. AFNI was used to map cortical and subcortical regions of interest. Metabolic rates were compared between three diagnostic groups using univariate and multivariate repeated-measures ANOVA.

Compared to controls, metabolic rates in schizophrenia subjects were decreased in the frontal lobe, anterior cingulate, superior temporal gyrus, amygdala and medial thalamic nuclei; rates were increased in the occipital cortex, hippocampus, basal ganglia and lateral thalamic nuclei. In ASD subjects metabolic rates were decreased in the parietal lobe, frontal premotor and eye-fields areas, and amygdala; rates were increased in the posterior cingulate, occipital cortex, hippocampus and basal ganglia. In relation to controls, subjects with ASD and schizophrenia showed opposite changes in metabolic rates in the primary motor and somatosensory cortex, anterior cingulate and hypothalamus; similar changes were found in prefrontal and occipital cortices, inferior parietal lobule, amygdala, hippocampus, and basal ganglia.

Schizophrenia and ASD appear to be associated with a similar pattern of metabolic abnormalities in the social brain. Divergent maladaptive trade-offs, as postulated by the diametrical hypothesis of their evolutionary relationship, may involve a more circumscribed set of anterior cingulate, motor and somatosensory regions and the specific cognitive functions they subserve.

Keywords

Autism spectrum disorder; Schizophrenia; Positron emission tomography; Fluorodeoxyglucose; Social brain; Diametrical diseases

Introduction

Recent developments in genome-wide association studies of psychiatric disorders have led to renewed interest in their interrelationships (Lee et al. 2013). This is particularly true of schizophrenia and autism spectrum disorders (ASD), which were among the last major psychiatric diagnoses to be nosologically separated, with ASD accorded its own set of formal diagnostic criteria in DSM-III (Hommer and Swedo 2015). Both are viewed as neurodevelopmental conditions (Rapoport, Giedd and Gogtay 2012) with prominent impairments in social cognition, and falling on a spectrum that fades into a population variance in normal psychological traits (Crespi and Badcock 2008). With a general consensus that disturbance of the social brain is a major feature of both disorders, the nature of this disturbance remains debatable and several distinct views on this can be discerned (Crespi, Stead and Elliot 2010). Various authors describe this shared involvement of the social brain as coincidental (due to etiologically unrelated pathological processes in each disorder, encompassing partially overlapping structures of the brain) (Bertone, Mottron, and Faubert 2004) or epiphenomenal (primary in schizophrenia, but only secondary in ASD and stemming from an ontogenetically earlier disturbance in primary sensory processing) (Elsabbagh and Johnson 2016). Still others consider the overlap to be predilect by selective evolutionary pressures, with each disorder representing an extreme case of a diametric trade-

off in population variance for cognitive sets of social and nonsocial abilities (Crespi and Go 2015). Neuroimaging techniques naturally lend themselves to exploration of the proposed models of the social brain and other impairments in schizophrenia and ASD as reflected in differential topological patterns and vectors of brain changes predicted by each model.

Two recent structural MRI studies, directly comparing subjects with schizophrenia and ASD, found opposite changes in both gray and white matter volumes in several brain regions in relation to healthy controls (Katz et al. 2016; Mitelman et al. 2016), consistent with the diametrical hypothesis of social brain involvement in each of the disorders (Crespi and Badcock 2008). While volumetric analyses appear well-suited for elucidation of evolutionary and developmental impacts on related cerebral structures, functional imaging techniques may be used to delineate more proximate patterns of differential, task-induced activation. Indeed, two such fMRI studies of ASD and schizophrenia lend support to the diametrical hypothesis (Ciaramidato et al. 2015; Abu-Akel et al. 2016) and another report implied a mere functional overlap (Yahata et al. 2016). [^{18}F]-fluorodeoxyglucose (FDG) PET, owing to the extended tracer uptake period, is uniquely positioned to evaluate between-group differences in more sustained task-dependent and basal metabolic patterns, thus occupying an intermediate space between structural and functional MRI. FDG-PET assessments of subjects with schizophrenia have consistently reported hypofrontality (especially in relation to negative symptoms), decreased metabolic rates in the prefrontal and anterior cingulate regions, as well as some thalamic nuclei (mediodorsal, pulvinar), lateralized changes in the temporal lobes, and increased metabolic rates in the basal ganglia (caudate, putamen, especially in relation to positive symptoms) (Buchsbaum and Hazlett 1998; Schöll, Damián and Engler 2014). Findings in ASD proved somewhat less consistent, generally pointing to diminished metabolic rates in the anterior cingulate, parietal cortex, basal ganglia (caudate, putamen), as well as increased metabolic rates in the occipital cortex (Zürcher et al. 2015; Hazlett et al. 2004). Only a single study directly compared subjects with schizophrenia and ASD during a continuous performance test, confirming decreased metabolism in the anterior cingulate and increased metabolism in the parietal regions in schizophrenia, as well as decreased metabolism in the medial thalamus in those with infantile autism (Siegel et al. 1995). In the present study, we used FDG PET during a modified California Verbal Learning Test to directly compare cortical and subcortical glucose metabolic rates in subjects with schizophrenia and ASD in relation to healthy controls. Topological patterns and vectors of metabolic activity were examined in order to investigate the nature of a proposed relationship between schizophrenia and ASD with respect to the above-referenced theoretical models. Our previous morphometric assessment on a sample of subjects with ASD and schizophrenia, overlapping with the present cohort, revealed a diametric relationship among gray matter volumes in these diagnostic groups in relation to healthy controls, with invariably larger volumes in those with ASD (Mitelman et al. 2016). We deemed these results strongly supportive of the Crespi and Badcock hypothesis (2008) and in turn hypothesized that this diametric relationship will be upheld by a comparable pattern of gray matter metabolism.

Methods

Participants

Study participants comprised 41 subjects with schizophrenia (age=40.0±18.0 years, 9 females), 25 subjects with ASD (age=31.48±11.57, 4 females), and 55 healthy controls (age=33.36±12.85, 26 females). Subjects with schizophrenia were recruited from the inpatient and outpatient services at Pilgrim State Psychiatric Center, Mount Sinai Hospital and the Bronx VA Medical Center in the New York metropolitan area. They varied in illness chronicity (duration of illness = 15.77±15.64 years, ranging from 1 to 59 years) and level of social functioning (14 with Kraepelinian schizophrenia subtype, 27 with non-Kraepelinian subtype, based on criteria of Keefe et al. 1987). PANSS scores were 19.14±7.0 (positive), 19.24±7.2 (negative) and 38.36±11.0 (general). Subjects with ASD were recruited by advertisements at the Seaver Autism Center at the Icahn School of Medicine at Mount Sinai. Diagnosis was confirmed by both DSM-IV criteria and Autism Diagnostic Interview-Revised. ASD subjects were verbal and were administered the WAIS and the Raven's Progressive Matrices (not available for 6 participants). The mean full-scale IQ score for the ASD group was 108.80±20.25 (verbal IQ=110.15±20.70, performance IQ=105.70±19.93). All ASD and schizophrenia participants were unmedicated with psychotropic substances for at least 14 days prior to scan date. Study participants in the present report were also part of our structural MRI comparison of subjects with schizophrenia and ASD (Mitelman et al. 2016) and of FDG PET comparison of subjects with Kraepelinian and non-Kraepelinian schizophrenia (Bralet et al. 2016), subsample of ASD subjects featured in Hazlett et al. (2004) and Haznedar et al. (2006). In comparison to the latter two studies, the present report employs a larger cohort of participants, analyzes different regions of interest with a newer automated region-of-interest approach.

Data acquisition and processing

All participants had a negative urine screen for drugs of abuse and all women also had a negative pregnancy test on scan day. An intravenous line was inserted into a forearm vein in each arm of the subject and kept patent by normal saline, 50–75 ml/h. The subject was instructed on the serial verbal learning task (SVLT) prior to isotope injection in the sound-attenuated uptake room in the Mount Sinai PET Center. The serial verbal learning task (see Hazlett et al. 2010 for task details) was initiated on a computer screen directly in front of the subject. Immediately upon starting the SVLT, 5 mCi of ^{18}FDG (185 Mbq) were administered into the venous set rubber diaphragm behind the subject's back as a 45–60 seconds slow push. The tube was clamped above the port before administration; after administration the saline was allowed to run at maximum rate for 6 minutes to flush the line, which was then closed. The subject remained in the uptake room and performed the SVLT for 32 minutes before being escorted to the adjacent bathroom to void, then positioned in the scanner using their own premolded thermosetting plastic mask. Imaging data acquisition lasted approximately 40 minutes. The PET scans were obtained with a head-dedicated scanner (GE Medical Systems model 2048) with measured resolution of 4.5 mm in plane (4.2–4.5 mm across 15 planes) and 5.0 mm axially. 15 slices at 6.5-mm intervals were obtained in two sets so as to cover the entire brain. Slice counts of 1.5–3 M were typical. Scans were reconstructed with a blank transmission scan and the Hann filter.

The SVLT, based on the principles of the California Verbal Learning Test (Delis et al. 1987), consists of five word lists containing 16 words each divided into 4 semantic categories (e.g., colors, animals, desserts, drinks). Each of the five lists is presented on a computer monitor five times at a rate of one word every 1.5 seconds, avoiding consecutive presentation of words from the same semantic category. Ordering of the words within each list, as well as the presentation order of each list were identical for all participants. The participants read each word aloud as it appeared on the computer monitor to maintain steady focus of attention on the task. After completion of each 16-word module, participants are asked to recall as many words as they remembered. Each list was repeated five times before moving to the next 16-word list. Responses were scored for total number of correctly recalled words, recall by semantic clustering, recall by serial order, intrusions, and perseverations; each of these scores was averaged across trials. The semantic clustering score was defined as the number of contiguously recalled correct words from the same semantic category, yielding a maximum potential score of 12 clustered words per list. The serial-order score was defined as the number of contiguously recalled items in the same relative order as presented on the list, yielding a maximum of 15 ordered words per list. Intrusions were defined as the number of words named that did not appear on the current word list, and perseverations were defined as the number of words repeated within the same trial.

T_1-weighted MR images were acquired using a 1.5T Signa 5× scanner (GE Medical Systems) with a 3D-SPGR sequence (TR=24 msec, TE=5 msec, flip angle=40°, matrix size=256×256, field of view=23 cm, slice thickness=1.2 mm, total slices=128, NEX=1). Anatomical SPGR MR images were resectioned to standard Talairach-Tournoux position using the protocol of Woods et al (1993) and a 6-parameter rigid-body transformation. For analyses of 42 cortical Brodmann areas and subcortical structures we obtained FDG uptake values using the AFNI regions of interest (Cox 1996). Only the structures featured in published literature on ASD and schizophrenia were chosen for analyses. These included the amygdala, hippocampus, cerebellar subregions (tonsil, culmen, declive, tuber, and pyramis of the vermis), basal ganglia associates structures (head, body and tail of the caudate, putamen, lateral globus pallidus, medial globus pallidus, red nucleus, substantia nigra, claustrum), mammillary body, hypothalamus, whole thalamus and thalamic nuclei (pulvinar, anteroventral, lateral dorsal, ventral lateral, ventral posteromedial, lateral posterior, ventroposterior lateral, mediodorsal, as well as the anterior and midline nuclear groups). We normalized the images by dividing each voxel value by the mean value of the whole brain, masked with the MNI brain and using slices above MNI z=-53. A restricted vertical range was chosen to minimize errors in the brain extraction routine at low slice levels. These relative metabolic rates were used in all analyses.

Statistical analyses

Repeated-measures ANCOVA (with subjects' age as a covariate) was used to ascertain significant patterns of differences in glucose metabolic rates among the three diagnostic groups and then for two-group comparisons (subjects with schizophrenia vs. subjects with ASD, subjects with schizophrenia vs. healthy controls, subjects with ASD vs. healthy controls). For cortical analyses, metabolic rates for each of the 42 Brodmann areas were entered into an ANCOVA with repeated measures of hemisphere and Brodmann areas. Main

effects of diagnosis, as well as higher-order group-by-hemisphere and group-by-Brodmann area interactions were assessed for hemispheric and localized intergroup differences in metabolic rates. These analyses of the whole cortex were followed by separate lobar analyses for constellations of Brodmann areas in each of the lobes, as well as the cingulate arch: 11 areas in the frontal lobe (4, 6, 8, 9, 10, 11, 12, 44, 45, 46, 47), 12 areas in the temporal lobe (20, 21, 22, 27, 28, 34, 35, 36, 37, 38, 41, 42), 8 areas in the parietal lobe (1, 2, 3, 5, 7, 39, 40, 43), 3 areas in the occipital lobe (17, 18, 19), and 8 areas in the cingulate (23, 24, 25, 29, 30, 31, 32, 33). In addition to univariate F, multivariate Wilks' λ statistics were documented for all higher-order (i.e. other than main effects) interactions. We selected the use of repeated measures MANOVA as our strategy to counteract the problem of multiple comparisons since it reduced their number to a single group-by-Brodmann area interaction, with visual assessment of the graphed patterns. For reference in the future replication studies, we do, however, report significant F statistics for follow-up three-group ANCOVAs on each of the individual Brodmann areas that emerge as differential in the inspection of the graphed patterns. Similar analyses were used for comparisons of relevant subcortical structures, with evaluation of main effects of diagnosis for all of them and also diagnostic group-by-region interaction for subregions of the caudate. Age was used as a covariate due to significant age differences among three groups of participants (ANOVA $F_{2, 118}=3.47$, $p=0.034$). We supplement these results (Tables 1 and 2) with ANOVAs without controlling for age as illustrated in Figures 1–4, because different age trajectories of ASD and schizophrenia may potentially render ANCOVA correction confounded. We report all 42 Brodmann areas and 16 subcortical structures to provide a systematic database (Table 1). Since earlier studies have tended to emphasize frontal, thalamic and striatal differences in subjects with schizophrenia and cingulate, parietal and cerebellar differences in ASD, a wide region of interest selection was important for the three-group analyses. Since a number of studies have reported multiple regions of significant differences in two-group analyses, we have reported uncorrected, Bonferroni corrected, and MANOVA repeated measures interactions to provide control of Type I and II error. We applied two strategies in correcting for multiple region testing and the problem of type I error. First, we entered the entire cortical dataset into an all-data ANOVA (42 Brodmann areas × three diagnostic groups × two hemispheres). If this was significant at the $p<0.05$ level, we then examined follow-up ANOVA for specific brain lobes considering main effect of group and group×Brodmann area interaction (two tests). However, since individual t-tests are most commonly reported in the literature we also examined follow-up group–pair ANOVA and t-tests. For patients vs. healthy controls comparison we computed the Bonferroni correction based on the number of variables in the cortex and subcortical regions separately because published literature values have been reported for single structures and single hemispheres, typically in separate reports. An alternative was to compute the denominator based on the three-group comparison and the three two-group comparisons (variables×4). However, this strategy could have been considered spuriously conservative since it would be associated with a false failure to replicate published findings. Therefore, we present all data both as $p<0.05$ as replication and Bonferroni corrected for multiple structures.

Results

Subjects with ASD and schizophrenia vs. healthy controls

Based on the three-group MANCOVA with repeated measures of hemisphere and Brodmann areas, comparing FDG metabolic rates across all 42 Brodmann areas in subjects with ASD, schizophrenia and healthy controls, there emerged a divergent pattern of greater-than-normal rates in those with schizophrenia and lower-than-normal rates in those with ASD in the precentral/postcentral region comprising areas 2, 3, 4, and 5 (Tables 1 and 2, Fig. 1). Follow-up analysis of the precentral/postcentral region confirmed significant intergroup differences (Fig. 2). The reversed pattern of greater-than-normal rates in ASD and lower-than-normal rates in schizophrenia was observed in the anterior cingulate (contiguous areas 33 and 32), to a lesser degree frontal area 9. Both subjects with schizophrenia and ASD showed lower-than-normal metabolic rates in a vast frontal region comprising areas 8, 10, 11, 45, 46, and 47 (more pronounced in those with schizophrenia), as well as contiguous parietal areas 39 and 40 (more pronounced in those with ASD). Both patient groups had higher-than-normal metabolic rates in occipital areas 17 and 18. Metabolic rates in postcentral areas 1 and 7 were decreased only in subjects with ASD and not in those with schizophrenia.

This overarching MANCOVA was followed by lobar analyses, which produced two significant main effects of diagnosis. In the frontal lobe (average for all 11 Brodmann areas), these results indicated lower metabolic rates in subjects with schizophrenia than in those with ASD and healthy controls (with no appreciable differences between the latter two groups). In the parietal lobe (average for all 8 Brodmann areas), significant main effect indicated lower metabolic rates in subjects with ASD than in those with schizophrenia and healthy controls (with no differences between the latter two groups). Diagnostic group-by-Brodmann area interactions confirmed patterns observed in the whole-cortex analysis for the frontal, parietal, and occipital lobes. In the frontal lobe, metabolic rates in subjects with schizophrenia were the lowest of three groups in all Brodmann areas, except area 4 (see Figures 3 and 4 for detailed analyses of the frontal lobe). In the parietal lobe, metabolic rates in subjects with ASD were the lowest of three groups in all areas, except area 43. Temporal lobe and cingulate gyrus analyses yielded no significant group-by-Brodmann area interactions.

In analyses of subcortical structures, a pattern of greater-than-normal rates in subjects with ASD and lower-than-normal rates in those with schizophrenia was observed only in the hypothalamus. A reverse pattern was not observed in any of the analyses. Both subjects with schizophrenia and ASD showed lower-than-normal metabolic rates in the amygdala, claustrum, and ventral posteromedial nucleus of the thalamus (in the latter more pronounced in subjects with schizophrenia). Both subjects with schizophrenia and ASD showed higher-than-normal metabolic rates in the lateral globus pallidus, putamen and pulvinar (more pronounced in those with schizophrenia); medial globus pallidus (more pronounced in those with ASD); tail of the caudate and hippocampus (equal increases in both groups). Only subjects with schizophrenia showed increased metabolic rates in the lateral posterior and ventroposterior lateral nuclei of the thalamus, and decreased metabolic rates in the head and body of the caudate (Fig. 5), and at a trend level also in the mediodorsal nucleus of the

thalamus. There were no significant interactions in three-group or any of the two-group analyses of the red nucleus, substantia nigra, cerebellar subregions (tonsil, culmen, declive, tuber, and pyramis of the vermis), whole thalamus and the following thalamic nuclei: anteroventral, lateral dorsal, ventral lateral, anterior and midline nuclear groups.

Direct two-group comparison of all 42 Brodmann areas in subjects with ASD and schizophrenia produced a trend-level group-by-area interaction, indicating a pattern of lower metabolic rates in subjects with ASD in the contiguous pericentral region (areas 1, 2, 3, 4, 5, 6, 7) and at the parieto-occipital junction (areas 39 and 40), and higher rates across the rest of the cortex; none of the lobar analyses yielded significant main effects of diagnosis. In subcortical analyses, only three structures yielded significant effects: in the hypothalamus and adjacent mammillary bodies rates were higher in subjects with ASD, in the lateral posterior nucleus of the thalamus rates were higher in those with schizophrenia. A significant group-by-hemisphere interaction for the amygdala pointed to higher metabolic rates in left than right hemisphere in subjects with schizophrenia, whereas there was an opposite pattern in those with ASD ($F_{1, 66}$ =6.29, p=0.015).

Subjects with ASD vs. healthy controls

The MANCOVA with all 42 Brodmann areas comparing subjects with ASD and healthy controls yielded a significant group-by-area interaction, indicating lower metabolic rates in subjects with ASD in most of parietal areas, as well as frontal areas 6, 8, and 11. Metabolic rates were higher in subjects with ASD in the posterior and pregenual cingulate (23, 29, 30, 33), occipital (17, 18) and inferior frontal cortices (area 12), and to a lesser degree in the medial temporal cortex (contiguous areas 27, 28, 34, 35, 36, 37, 38). Differential metabolic patterns on the lobar level were confirmed only in the parietal lobe analysis (main effect of diagnosis), with lower metabolic rates in subjects with ASD across all areas, except area 43.

In subcortical analyses, subjects with ASD showed increased metabolic rates in the putamen, medial and lateral globi pallidi, tail of the caudate, claustrum, and hippocampus. In comparison to healthy controls, metabolic rates were decreased only in the amygdala.

Subjects with schizophrenia vs. healthy controls

In comparisons of subjects with schizophrenia and healthy controls, significant group-by-Brodmann area interactions were obtained for the overarching 42 Brodmann area MANCOVA and in analyses of the frontal, parietal and occipital lobes. These indicated lower metabolic rates in subjects with schizophrenia in all frontal areas, except precentral area 4, and in the parietal area 40 (supramarginal gyrus), superior temporal gyrus (area 22), and in the primarily anterior cingulate gyrus (areas 25, 32, 33, to lesser degree 23 and 24). Significant main effect of diagnosis confirmed lower metabolic rates in those with schizophrenia in the whole frontal lobe. Higher-than-normal rates in subjects with schizophrenia were seen in the occipital areas 17 and 18. In subcortical analyses, subjects with schizophrenia showed increased metabolic rates in the lateral globus pallidus, putamen, tail of the caudate, claustrum, hippocampus, as well as the pulvinar, ventroposterior lateral and lateral posterior nuclei of the thalamus. Metabolic rates were decreased in the

hippocampus, amygdala, head of the caudate, and in the mediodorsal and ventral posteromedial nuclei of the thalamus.

In t-tests on 42 individual Brodmann areas for right and left hemispheres, areas 10L, 10R, 44R, 45R, 47R and 47L met the Bonferroni criterion (0.05/84=0.00060) in schizophrenia vs. healthy controls comparisons; only area 1R met this criterion in ASD vs. healthy controls comparisons. The largest effect size for any Brodmann area metabolic rates for healthy controls vs. schizophrenia comparisons was in right area 44 (t_{94}=4.20, effect size=0.86, p=0.000061; schizophrenia 1.23±0.087, healthy controls 1.29±0.070). This area met Bonferroni criterion (0.05/84, p=0.00060) for subjects with schizophrenia, but it was not significant (p<0.05) in ASD vs. healthy controls comparison.

Serial Verbal Learning Test

Based on Student's t-tests, subjects with schizophrenia showed worse performance than healthy controls in total number of correctly memorized words (t_{89}=11.18, p<0.0000001) and in their semantic clustering (t_{89}=9.57, p<0.0000001), and they expressed more intrusions (t_{89}=3.53, p=0.0007) and perseverations (t_{89}=3.10, p=0.003), with no significant differences in serial ordering (Fig. 6). Subjects with ASD showed worse performance than healthy controls in semantic clustering (t_{60}=2.32, p=0.02) and more intrusions (t_{61}=3.50, p=0.0009) and perseverations (t_{61}=2.30, p=0.025), but their performance was numerically intermediate to that of healthy controls and subjects with schizophrenia. In direct comparison of subjects with ASD and schizophrenia, the latter showed worse performance in total number of correctly memorized words (t_{43}=3.74, p=0.0005) and in their semantic clustering (t_{43}=2.38, p=0.02).

In order to test whether between-group differences in metabolic rates were primarily related to differential activation under task performance, we ran three-group and two-group ANCOVAs controlling for performance on the two SVLT subtests that showed significant differences between subjects with schizophrenia and ASD (number of correctly memorized words and semantic clustering). This was expected to render metabolic differences related to task-induced activations less or nonsignificant while leaving the regional differences in basal metabolic rates intact. After controlling for test performance in three-group analyses (schizophrenia, ASD, healthy controls) statistically significant, albeit diminished differences remained in the group-by-Brodmann area interaction for all 42 cortical Brodmann areas ($F_{82, 4059}$=1.60, p=0.0055, Wilks' λ p=0.006), as well as in main effects of diagnostic group for the hippocampus ($F_{2, 99}$= 6.89, p=0.002), claustrum ($F_{2, 99}$= 5.95, p=0.004), tail of the caudate nucleus ($F_{2, 99}$=9.10, p=0.0002), putamen ($F_{2, 99}$=3.75, p=0.03), lateral globus pallidus ($F_{2, 99}$ =3.33, p=0.04), and the thalamic nuclei: lateral posterior ($F_{2, 99}$=7.17, p=0.001), pulvinar ($F_{2, 99}$=5.26, p=0.007), and ventral posterolateral ($F_{2, 99}$=2.95, p=0.057, trend level). Differences in the hypothalamus and amygdala were reduced to the trend level of significance ($F_{2, 99}$=2.51, p=0.09 and $F_{2, 99}$=2.45, p=0.09, respectively). In two-group analyses (schizophrenia vs ASD) significant differences remained in the hypothalamus ($F_{1, 46}$=5.80, p=0.02) and posterolateral nucleus of the thalamus ($F_{1, 46}$=6.86, p=0.01), with trend level reached in the pulvinar ($F_{1, 46}$=3.24, p=0.08). Cortical Brodmann area ANCOVAs with SVLT scores as the covariates also produced significant group-by-hemisphere

interactions ($F_{2, 99}$=3.56, p=0.03 for three groups and $F_{1, 46}$=4.96, p=0.03 for two groups). These hemispheric effects pointed to greater-than-normal basal cortical metabolic rates in subjects with ASD and markedly lower-than-normal rates in those with schizophrenia in the right hemisphere, with much smaller between-group differences in the left hemisphere. Of the differences remaining statistically significant after controlling for task performance, all but the putamen and lateral globus pallidus survived the Bonferroni correction in three-group analyses, while none of the differences survived the procedure in two-group schizophrenia vs. ASD analyses (see footnotes to Table 1 for the Bonferroni criteria).

Exploratory analysis of correlation patterns between the subjects' performance on total number of correctly memorized words and their semantic clustering with metabolic rates across the regions of interest in each group of participants revealed the following intergroup differences. In healthy controls, significant positive correlations ($p<0.05$) for the total number of correctly memorized words were observed with the widespread cortical Brodmann areas in the left hemisphere (frontal areas 9, 10, 32; temporal areas 21, 22, 41; occipital area 19); negative correlations were recorded for the bilateral cerebellar subregions (uvula, tuber, pyramis) and right medial and lateral globi pallidi. Semantic clustering scores were positively correlated with metabolic rates in the left hemisphere Brodmann areas 9, 44 (frontal lobe) and 21, 22 (temporal lobe); negative correlations were recorded with the bilateral cerebellar subregions (tuber, pyramis, declive, culmen) and right medial and lateral globi pallidi. In subjects with schizophrenia, the total number of correctly memorized words yielded a single positive (left area 11) and negative (right cerebellar uvula) correlation; semantic clustering yielded positive correlations with bilateral area 11 and left area 25 (frontal lobe), and negative correlations with cerebellar subregions (right uvula and pyramis, left culmen) and right mediodorsal nucleus of the thalamus. In subjects with ASD, the total number of correctly memorized words was positively correlated with the left hemisphere areas 22, 37 (temporal lobe), bilateral areas 39, 42, 43 (parietal lobe and auditory cortex), as well as bilateral caudate (tail and body) and thalamic nuclei (right midline and pulvinar, left lateral dorsal); negative correlations were registered with the left cerebellar pyramis, temporal pole (area 38) and bilateral hypothalamus. Semantic clustering was positively correlated with the left hemisphere areas 8 (frontal lobe), 22, 42 (temporal lobe) and 43 (parietal lobe), bilateral caudate (tail and body), and thalamic nuclei (right lateral posterior and pulvinar, left midline); negative correlations were registered with the left temporal pole (area 38) and mammillary body, bilateral hypothalamus, and right substantia nigra.

Discussion

The main findings of this study, as pertains to direct comparison of subjects with schizophrenia and ASD, are twofold: 1) both groups displayed comparable deviations from the normal metabolic patterns in most of the regions generally associated with the so-called social brain; 2) divergent metabolic patterns, that are compatible with the hypothesis of ASD and schizophrenia as diametrical trade-off diseases, were confined to a much more limited assortment of structures, of which only the anterior cingulate, somatosensory and motor regions are tentatively accorded roles in social cognition.

Subjects with schizophrenia and ASD showed similar changes in metabolic rates in the prefrontal cortex, including the frontopolar, dorsolateral and orbitofrontal regions (areas 8, 10, 11, 44, 45, 46, 47), inferior parietal lobule at the temporoparietal junction (39, 40), primary and accessory visual areas in the occipital cortex (17, 18), amygdala, hippocampus, as well as two thalamic nuclei (pulvinar, ventral posteromedial) and basal ganglia associated structures (tail of the caudate, lateral and medial globi pallidi, claustrum, putamen). Most of these regions are viewed as major components of the social brain owing to such socially relevant functions as value assignment and more specifically emotion recognition (amygdala), theory of mind and perspective taking (temporoparietal junction, dorsolateral and ventromedial prefrontal cortex), mentalizing (medial prefrontal cortex), social reward (striatum) (Frith 2007; Adolphs 2009; Báez-Mendoza and Schultz 2013). Other shared regions point to similar impairments in visual information processing (occipital lobes), memory formation and retrieval (hippocampus), perseverative and stereotypical behaviors (basal ganglia).

Diametrically different changes in subjects with schizophrenia and ASD were found in the pericentral somatosensory and motor cortex (areas 2, 3, 4, 5), anterior cingulate (areas 32, 33), frontal area 9, and hypothalamus. Although still debated (Otti, Wohlschlaeger and Noll-Hussong 2015), motivational mechanisms and reward anticipation in the anterior cingulate and mirroring functions (empathy) of the motor and somatosensory cortices are often deemed relevant to social cognition and thus considered a part of the social brain (Frith 2007; Apps, Rushworth and Chang 2016). Medial portion of Brodmann area 9 may be relevant to reasoning, including social reasoning and mentalizing (Overwalle 2011; Hartwright, Apperly and Hansen 2014). In line with the diametrical hypothesis of Crespi and Badcock (2008), our present finding of higher-than-normal metabolic rates in the somatosensory and motor cortex in schizophrenia may underlie its position at the empathizing extreme of the systemizing-empathizing axis (Baron-Cohen 2009). The finding of higher-than-normal metabolic rates in the medial prefrontal cortex (area 9) in ASD may then underlie its position at the systemizing (over-reasoning) extreme (Stevenson and Gernsbacher 2013; Brosnan, Lewton and Ashwin 2016). Another intriguing possibility may arise if the regions with diametrical changes in metabolic rates in subjects with ASD and schizophrenia are considered as a network. Indeed, recent meta-analyses of PET imaging studies of dimorphism in male and female sexual behaviors include premotor and supplementary motor areas in their cognitive component, primary and secondary somatosensory areas – in the emotional component, anterior cingulate and hypothalamus – in the motivational component (Stoléru et al. 2012). Of these, increased metabolic rates in the hypothalamus appear exclusively correlated with male sexual response (Poeppl et al. 2016). The extreme male brain theory of autism (Baron-Cohen, Knickmeyer and Belmonte 2005; Baron-Cohen 2010) posits the systemizing–empathizing axis of cognitive styles as a function of the dimensional distribution of psychological correlates of sexual dimorphism in population. Herein reported higher-than-normal metabolic rates in the hypothalamus in subjects with ASD, as predicted by the extreme male brain theory, would place them at the male brain extreme, and reverse would be true of those with schizophrenia. Intergroup differences in the motor, somatosensory, medial frontal and anterior cingulate areas may be interpreted in the same vein, with diametrical cognitive styles of the two disorders viewed as

secondary to their positions along the axis of distribution of sex differences in brain morphology in the general population.

Finally, regions where only one of the diagnostic groups showed differential metabolic patterns included the superior parietal lobule, caudate head and body, and 3 thalamic nuclei (lateral posterior, ventroposterior lateral, and mediodorsal). These structures may therefore underlie unique clinical features of each of the disorders. Other findings in this study point to hemispheric differences between subjects with ASD and schizophrenia in the amygdalar activation and the more pronounced right than left hemisphere differences in basal cortical metabolic rates.

Our previous morphometric investigation on an overlapping cohort of participants (Mitelman et al. 2016) allows for a comparison of changes in gray matter volumes (adjusted for total brain volume) and co-territorial glucose metabolism. While in the anterior cingulate cortex and frontal Brodmann area 9 both the volumes and metabolic rates where greater-than-normal in subjects with ASD and lower-than-normal in those with schizophrenia, an inverse relationship between volumes and metabolism was seen in the precentral/postcentral (motor and somatosensory) region. In this latter region, volumes were greater-than-normal in ASD and lower-than-normal in schizophrenia, but metabolic rates were lower-than-normal in ASD and greater-than-normal in schizophrenia. This suggests that direction of changes in cerebral metabolism cannot be reliably predicted from concurrent changes in cerebral volumes. Larger regional volumes may still have the same number of neurons in a less dense array resulting in a lower relative metabolic rate.

Schizophrenia

Compared to healthy controls, subjects with schizophrenia displayed a pattern of hypofrontality, with decreased glucose metabolism in the whole frontal lobe, as well as superior temporal gyrus, anterior cingulate cortex and amygdala. Increased metabolic rates were seen in the occipital visual cortex, basal ganglia associated structures (lateral globus pallidus, tail of the caudate, putamen, claustrum), as well as the hippocampus, where many studies have previously found basal hyperperfusion in schizophrenia (reviewed in Tamminga et al. 2010).

A gradient of metabolic activity was observed in the caudate (decreased rates in the head, increased rates in the tail, and normal rates in the body), as well as the thalamus, where rates were decreased in two medial thalamic nuclei (mediodorsal and ventral posteromedial) and increased in lateral nuclei (ventroposterior lateral, lateral posterior and pulvinar). Other PET studies have similarly reported decreased metabolic rates in the mediodorsal and centromedian nuclei, and increased rates in the pulvinar, as well as abnormal connectivity patterns of these structures (Hazlett et al. 2004; Mitelman et al. 2005; Lehrer et al. 2005), but no gradient of metabolic activity within the thalamus has previously been suggested. An upward rostrocaudal gradient of glucose metabolism in the caudate in schizophrenia may be evidence of an accentuation of the normally occurring rostrocaudal increment in the density of D_2 receptors and dopamine uptake sites in this nucleus (Piggott et al. 1999).

Autism

As compared to healthy controls, subjects with ASD displayed lower metabolic rates in the whole parietal lobe, as well as the frontal premotor/supplementary motor and eye-fields areas, rostral orbitofrontal cortex, and amygdala. Increased metabolic rates were found in the posterior cingulate and occipital visual cortices, orbitofrontal area 12, and medial temporal cortex, as well as the hippocampus and basal ganglia associated structures (medial and lateral globi pallidi, tail of the caudate, claustrum and putamen). In contrast to some prior reports, we found no metabolic changes in the cerebellum or any of its subdivisions.

Similar to our present findings, amygdalar hypoactivation has been a common thread in recent fMRI investigations in ASD (Dichter 2012). Caudate and lentiform nuclei impairments, among other structures, were found in an early ^{18}FDG PET intercorrelations study (Horwitz et al. 1988) and caudate hyperactivation emerged as the most robust finding in a meta-analysis of fMRI studies with emotional face processing tasks (Aoki, Cortese and Tansella 2015). A small [1-^{11}C]butanol PET study likewise observed hyperperfusion in the caudate and putamen, as well as the posterior cingulate gyrus (Pagani et al. 2012). In contrast, decreased metabolic rates in the ventral caudate and putamen were found in one ^{18}FDG PET study (Haznedar et al. 2006) and in the left posterior putamen only in another ^{18}FDG PET study (Siegel et al. 1992).

Increased metabolic rates in the posterior cingulate cortex could reflect diminished cognitive task engagement of subjects with ASD, which in healthy participants typically leads to lowered metabolic activity in this region (Pfefferbaum et al. 2011) – central to the default mode network (Leech and Sharp 2013). However, while altered task-related deactivation of the posterior cingulate cortex has been previously shown using fMRI in schizophrenia (Harrison et al. 2007; Whitfield-Gabrieli et al. 2009), our findings are confined to ASD and not schizophrenia. It is therefore likely that rather than being due to diminished cognitive task engagement metabolic hyperactivity of the posterior cingulate connotes an inefficient overall functioning of the default network in ASD. In particular, greater metabolic resources are devoted to the maintenance of a cohesive sense of self (functionally attributed to the posterior cingulate cortex, see Davey, Pujol and Harison 2016), which some theorists view as the central impairment in the phenomenology of autism (Glezerman 2013).

Cognitive task performance

Subjects with schizophrenia and ASD differed in their performance on two of the administered cognitive tasks (total number of correctly memorized words and their semantic clustering), and controlling for these subscores in main analyses of variance showed that the between-group patterns of regional differences reported in this study were due to the combination of differences in both the task-induced activations and basal metabolic rates. Exploratory correlation analyses suggested that while in healthy controls better task performance was associated with greater activations across the wide network of cortical regions in the left hemisphere and suppression of the cerebellar and pallidal metabolism, these patterns were disturbed in both patient groups. We observed a paucity of both positive and negative significant correlations of metabolic rates and task performance in subjects with schizophrenia in the cortical and subcortical structures. In subjects with ASD, on the

other hand, we saw a diminished association of better task performance with cortical activations, with involvement of the subcortical structures (nuclei of the thalamus and caudate) instead, as well a conspicuous reliance on metabolic suppression of the hypothalamus and adjacent mammillary bodies rather than the globus pallidus and cerebellum as in healthy controls.

Limitations

The following limitations and caveats of this study have to be considered in interpretation of its results. Schizophrenia subjects in this cohort reflect a wide gamut of illness severity, chronicity and social functioning, comprising inpatient and outpatient, as well as good-outcome and poor-outcome participants. In contrast, subjects with ASD are invariably high-functioning, with no concurrent intellectual disability or pharmacological anamnesis, i.e. clearly a minority of those within the spectrum and nowhere near its more severe extreme. This may potentially efface some of the diametrical differences in metabolic rates, but is not expected to impact on their similarities and topological overlaps. Secondly, functional neuroimaging activation patterns are inherently influenced by a choice of cognitive tasks, in this case the modified California Verbal Learning Test. The latter invokes a broad range of cognitive demands, including memory, learning, comprehension of both verbal and written language, as well as auditory and visual information processing, but it's not specifically geared towards emotion recognition and processing, face perception, elicitation of empathic responses, mental state attribution and theory of mind, – all prominent in the semiotics of both disorders. This may potentially de-emphasize such pertinent regions as the fusiform gyrus, amygdala–orbitofrontal network and mirroring system, but – of all functional imaging techniques – the long tracer uptake period of ^{18}FDG PET tends to mitigate this problem by averaging the 30 minute task-induced changes in metabolic rates and thus shifting emphasis to the basal metabolic activity.

Acknowledgments

This work was partly supported by NARSAD Young Investigator Award and NIMH MH 077146 grant to Serge A. Mitelman and by NIMH grants P50 MH 66392-01, MH 60023, and MH 56489 to Monte S. Buchsbaum.

References

Abu-Akel AM, Apperly IA, Wood SJ, Hansen PC. Autism and psychosis expressions diametrically modulate the right temporoparietal junction. Social Neuroscience. 2016:1–13.

Adolphs R. The social brain: neural basis of social knowledge. Annual Review of Psychology. 2009; 60:693–716.

Aoki Y, Cortese S, Tansella M. Neural bases of atypical emotional face processing in autism: a meta-analysis of fMRI studies. World Journal of Biological Psychiatry. 2015; 16(5):291–300. [PubMed: 25264291]

Apps MA, Rushworth MF, Chang SW. The anterior cingulate gyrus and social cognition: tracking the motivation of others. Neuron. 2016; 90(4):692–707. [PubMed: 27196973]

Báez-Mendoza R, Schultz W. The role of the striatum in social behavior. Frontiers of Neuroscience. 2013; 7:233.

Baron-Cohen S. Autism: the empathizing-systemizing (E-S) theory. Annals of New York Academy of Sciences. 2009; 1156:68–80.

Baron-Cohen S. Empathizing, systemizing, and the extreme male brain theory of autism. Progress in Brain Research. 2010; 185:167–175. [PubMed: 21075239]

Baron-Cohen S, Knickmeyer RC, Belmonte MK. Sex differences in the brain: implications for explaining autism. Science. 2005; 310:819–823. [PubMed: 16272115]

Bertone A, Mottron L, Faubert J. Autism and schizophrenia: Similar perceptual consequence, different neurobiological etiology? Behavioral and Brain Sciences. 2004; 27(4):592–593.

Bralet MC, Buchsbaum MS, DeCastro A, Hazlett EA, Haznedar MM, Shihabuddin L, Mitelman SA. FDG-PET scans in patients with Kraepelinian and non-Kraepelinian schizophrenia. European Archives of Psychiatry and Clinical Neurosciences. 2016; 266(6):481–494.

Brosnan M, Lewton M, Ashwin C. Reasoning on the autism spectrum: a dual process theory account. Journal of Autism and Developmental Disorders. 2016; 46:2115–2125. [PubMed: 26960339]

Buchsbaum MS, Hazlett EA. Positron emission tomography studies of abnormal glucose metabolism in schizophrenia. Schizophrenia Bulletin. 1998; 24(3):343–364. [PubMed: 9718628]

Ciaramidaro A, Bölte S, Schlitt S, Hainz D, Poustka F, Weber B, Bara BG, Freitag C, Walter H. Schizophrenia and autism as contrasting minds: neural evidence for the hypo-hyper-intentionality hypothesis. Schizophrenia Bulletin. 2015; 41(1):171–179. [PubMed: 25210055]

Cox RW. AFNI: software for analysis and visualization of functional magnetic resonance neuroimages. Computers and Biomedical Research. 1996; 29(3):162–173. [PubMed: 8812068]

Crespi BJ, Badcock C. Psychosis and autism as diametrical disorders of the social brain. Behavioral and Brain Sciences. 2008; 31(3):241–161. [PubMed: 18578904]

Crespi BJ, Go MC. Diametrical diseases reflect evolutionary-genetic tradeoffs: Evidence from psychiatry, neurology, rheumatology, oncology and immunology. Evolution, Medicine and Public Health. 2015; 2015(1):216–253.

Crespi B, Stead P, Elliot M. Comparative genomics of autism and schizophrenia. Proceedings of the National Academy of Sciences of the United States of America. 2010; 107(Suppl 1):1736–1741. [PubMed: 19955444]

Davey CG, Pujol J, Harrison BJ. Mapping the self in the brain's default mode network. NeuroImage. 2016; 132:390–397. [PubMed: 26892855]

Delis, D., Kramer, J., Kaplan, E., Ober, B. The California Verbal Learning Test. Psychological Corporation; New York: 1987.

Dichter GS. Functional magnetic resonance imaging of autism spectrum disorders. Dialogues in Clinical Neuroscience. 2012; 14(3):319–351. [PubMed: 23226956]

Elsabbagh M, Johnson MH. Autism and the social brain: the first-year puzzle. Biological Psychiatry. 2016; 80(2):94–99. [PubMed: 27113503]

Frith CD. The social brain? Philosophical Transactions of the Royal Society of London, Series B Biological Sciences. 2007; 362(1480):671–678. [PubMed: 17255010]

Glezerman, TB. Autism and the brain: Neurophenomenological interpretation. New York: Springer; 2013. p. 194p. 228-231.

Harrison BJ, Yücel M, Pujol J, Pantelis C. Task-induced deactivation of midline cortical regions in schizophrenia assessed with fMRI. Schizophrenia Research. 2007; 91(1–3):82–86. [PubMed: 17307337]

Hartwright CE, Apperly IA, Hansen PC. Representation, control, or reasoning? Distinct functions for theory of mind within the medial prefrontal cortex. Journal of Cognitive Neuroscience. 2014; 26(4):683–698. [PubMed: 24236763]

Hazlett EA, Buchsbaum MS, Hsieh P, Haznedar MM, Platholi J, LiCalzi EM, Cartwright C, Hollander E. Regional glucose metabolism within cortical Brodmann areas in healthy individuals and autistic patients. Neuropsychobiology. 2004; 49(3):115–125. [PubMed: 15034226]

Hazlett EA, Buchsbaum MS, Kemether E, Bloom R, Platholi J, Brickman AM, Shihabuddin L, Tang C, Byne W. Abnormal glucose metabolism in the mediodorsal nucleus of the thalamus in schizophrenia. American Journal of Psychiatry. 2004; 161(2):305–314. [PubMed: 14754780]

Hazlett EA, Byne W, Brickman AM, Mitsis EM, Newmark R, Haznedar MM, Knatz DT, Chen AD, Buchsbaum MS. Effects of sex and normal aging on regional brain activation during verbal memory performance. Neurobiology of Aging. 2010; 31(5):826–838. [PubMed: 19027195]

Haznedar MM, Buchsbaum MS, Hazlett EA, LiCalzi EM, Cartwright C, Hollander E. Volumetric analysis and three-dimensional glucose metabolic mapping of the striatum and thalamus in patients with autism spectrum disorders. American Journal of Psychiatry. 2006; 163(7):1252–1263. [PubMed: 16816232]

Hommer RE, Swedo SE. Schizophrenia and autism – related disorders. Schizophrenia Bulletin. 2015; 41(2):313–314. [PubMed: 25634913]

Horwitz B, Rumsey JM, Grady CL, Rapoport SI. The cerebral metabolic landscape in autism. Intercorrelations of regional glucose utilization. Archives of Neurology. 1988; 45(7):749–755. [PubMed: 3260481]

Katz J, d'Albis MA, Boisgontier J, Poupon C, Mangin JF, Guevara P, Duclap D, Hamdani N, Petit J, Monnet D, Le Corvoisier P, Leboyer M, Delorme R, Houenou J. Similar white matter but opposite grey matter changes in schizophrenia and high-functioning autism. Acta Psychiatrica Scandinavica. 2016; 134(1):31–39. [PubMed: 27105136]

Keefe RS, Mohs RC, Losonszy MF, Davidson M, Silverman JM, Kendler KS, Horvath TB, Nora R, Davis KL. Characteristics of very poor outcome schizophrenia. American Journal of Psychiatry. 1987; 144:889–895. [PubMed: 3605400]

Lee SH, Ripke S, Neale BM, Faraone SV, et al. Genetic relationship between five psychiatric disorders estimated from genome-wide SNPs. Nature Genetics. 2013; 45(9):984–994. [PubMed: 23933821]

Leech R, Sharp DJ. The role of the posterior cingulate cortex in cognition and disease. Brain. 2014; 137(1):12–32. [PubMed: 23869106]

Lehrer DS, Christian BT, Mantil J, Murray AC, Buchsbaum BR, Oakes TR, Byne W, Kemether EM, Buchsbaum MS. Thalamic and prefrontal FDG uptake in never medicated patients with schizophrenia. American Journal of Psychiatry. 2005; 162(5):931–938. [PubMed: 15863795]

Mitelman SA, Bralet M-C, Haznedar MM, Hollander E, Shihabuddin L, Hazlett EA, Buchsbaum MS. Diametrical relationship between gray and white matter volumes in autism spectrum disorder and schizophrenia. Brain Imaging and Behavior. 2016; doi: 10.1007/s11682-016-9648-9

Mitelman SA, Byne W, Kemether EM, Hazlett EA, Buchsbaum MS. Metabolic disconnection between the mediodorsal nucleus of the thalamus and cortical Brodmann's areas of the left hemisphere in schizophrenia. American Journal of Psychiatry. 2005; 162(9):1733–1735. [PubMed: 16135634]

Otti A, Wohlschlaeger AM, Noll-Hussong M. Is the medial prefrontal cortex necessary for theory of mind? PLoS One. 2015; 10(8)

Pagani M, Manouilenko I, Stone-Elander S, Odh R, Salmaso D, Hatherly R, Brolin F, Jacobsson H, Larsson SA, Bejerot S. Brief report: alterations in cerebral blood flow as assessed by PET/CT in adults with autism spectrum disorder with normal IQ. Journal of Autism and Developmental Disorders. 2012; 42(2):313–318. [PubMed: 21487836]

Pfefferbaum A, Chanraud S, Pitel AL, Müller-Oehring E, Shankaranarayanan A, Alsop DC, Rohlfing T, Sullivan EV. Cerebral blood flow in posterior cortical nodes of the default mode network decreases with task engagement but remains higher in most brain regions. Cerebral Cortex. 2011; 21(1):233–244. [PubMed: 20484322]

Piggott MA, Marshall EF, Thomas N, Lloyd S, Court JA, Jaros E, Costa D, Perry RH, Perry EK. Dopaminergic activities in the human striatum: rostrocaudal gradients of uptake sites and of D_1 and D_2 but not of D_3 receptor binding or dopamine. Neuroscience. 1999; 90(2):433–445. [PubMed: 10215149]

Poeppl TB, Langguth B, Rupprecht R, Safron A, Bzdok D, Laird AR, Eickhoff SB. The neural basis of sex differences in sexual behavior: a quantitative meta-analysis. Frontiers in Neuroendocrinology. 2016; 3022(16):28–43.

Rapoport JL, Giedd JN, Gogtay N. Neurodevelopmental model of schizophrenia: update 2012. Molecular Psychiatry. 2012; 17(12):1228–1238. [PubMed: 22488257]

Schöll M, Damián A, Engler H. Fluorodeoxyglucose PET in neurology and psychiatry. PET Clinics. 2014; 9(4):371–390. [PubMed: 26050943]

Siegel BV Jr, Asarnow R, Tanguay P, Call JD, Abel L, Ho A, Lott I, Buchsbaum MS. Regional cerebral glucose metabolism and attention in adults with a history of childhood autism. Journal of Neuropsychiatry and Clinical Neurosciences. 1992; 4(4):406–414. [PubMed: 1422167]

Siegel BV Jr, Nuechterlein KF, Abel L, Wu JC, Buchsbaum MS. Glucose metabolic correlates of continuous performance test performance in adults with a history of infantile autism, schizophrenia, and controls. Schizophrenia Research. 1995; 17(1):85–94. [PubMed: 8541254]

Stevenson JL, Gernsbacher MA. Abstract spatial reasoning as an autistic strength. PLoS One. 2013; 8(3):e59329. [PubMed: 23533615]

Stoléru S, Fonteille V, Cornélis C, Joyal C, Moulier V. Functional neuroimaging studies of sexual arousal and orgasm in healthy men and women: a review and meta-analysis. Neuroscience and Behavioral Reviews. 2012; 36:1481–1509.

Tamminga CA, Stan AD, Wagner AD. The hippocampal formation in schizophrenia. American Journal of Psychiatry. 2010; 167(10):1178–1193. [PubMed: 20810471]

van Overwalle F. A dissociation between social mentalizing and general reasoning. NeuroImage. 2011; 54(2):1589–1599. [PubMed: 20869452]

Whitfield-Gabrieli S, Thermenos HW, Milanovic S, Tsuang MT, Faraone SV, McCarley RW, Shenton ME, Green AI, Nieto-Castanon A, LaViolette P, Wojcik J, Gabrieli JD, Seidman LJ. Hyperactivity and hyperconnectivity of the default network in schizophrenia and in first-degree relatives of persons with schizophrenia. Proceedings of the National Academy of Sciences of the United States of America. 2009; 106(11):4572.

Woods RP, Mazziotta JC, Cherry SR. MRI-PET registration with automated algorithm. Journal of Computer Assisted Tomography. 1993; 17:536–546. [PubMed: 8331222]

Yahata N, Morimoto J, Hashimoto R, Lisi G, Shibata K, Kawakubo Y, Kuroda M, Yamada T, Megumi F, Imamizu H, Nañez JESr, Takahashi H, Okamoto Y, Kasai K, Kato N, Sasaki Y, Wanatabe T, Kawato M. A small number of abnormal brain connections predicts adult autism spectrum disorder. Nature Communications. 2016; 14(7):11254.

Zürcher NR, Bhanot A, McDougle CJ, Hooker JM. A systematic review of molecular imaging (PET and SPECT) in autism spectrum disorder: current state and future research opportunities. Neuroscience and Biobehavioral Reviews. 2015; 52:56–73. [PubMed: 25684726]

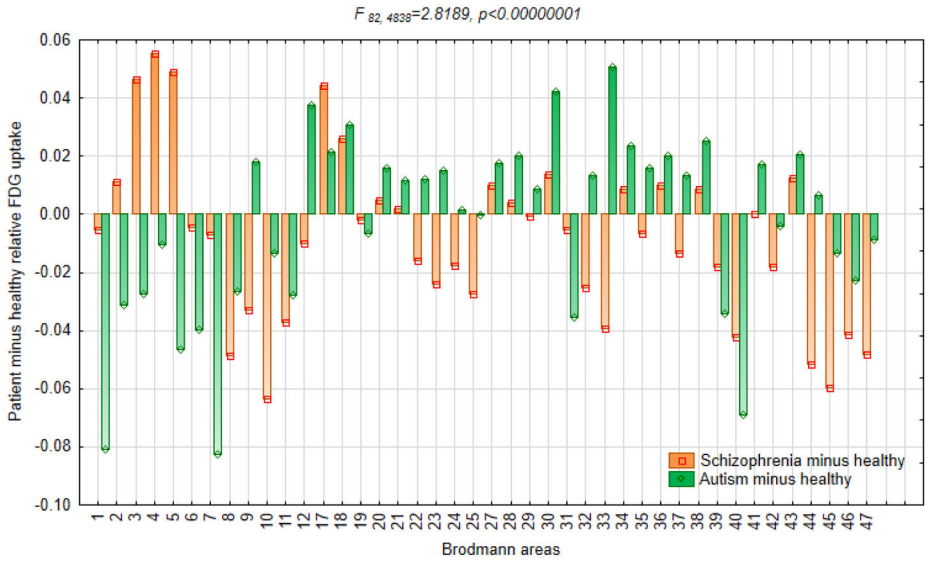

Figure 1.

Relative ^{18}fluorodeoxyglucose uptake in subjects with schizophrenia, subjects with ASD and healthy controls.

This graph is based on the diagnostic group-by-Brodmann area interaction in ANOVA with three diagnostic groups and 42 Brodmann areas. Orange and green bars represent metabolic rates in healthy controls subtracted from metabolic rates in subjects with autism and schizophrenia respectively, so that each patient group is plotted against the zero axis line of healthy controls.

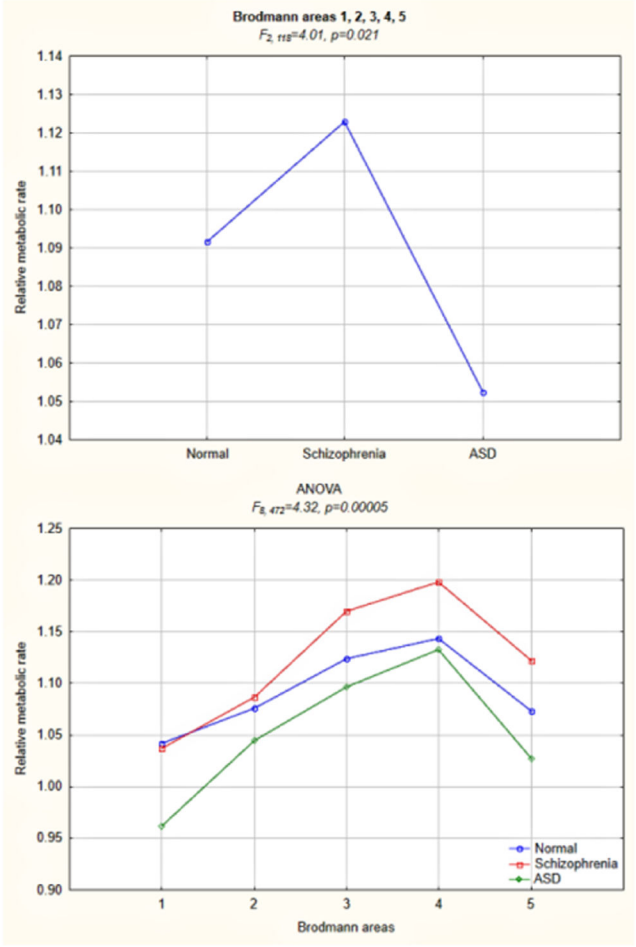

Figure 2.

Follow-up three-group ANOVA for a precentral/postcentral region comprising primary motor and somatosensory Brodmann areas 1, 2, 3, 4, and 5.

This figure illustrates the main effect of diagnostic group (upper panel) and group-by-Brodmann area interaction (lower panel) for the region where diametric differences between subjects with schizophrenia and ASD were observed in the overarching analysis of all 42 Brodmann areas. There were also significant main effects in two-group ANOVA for schizophrenia vs. healthy control ($F_{1, 94}$=6.86, p=0.01) and schizophrenia vs. ASD ($F_{1, 64}$=4.87, p=0.03) comparisons.

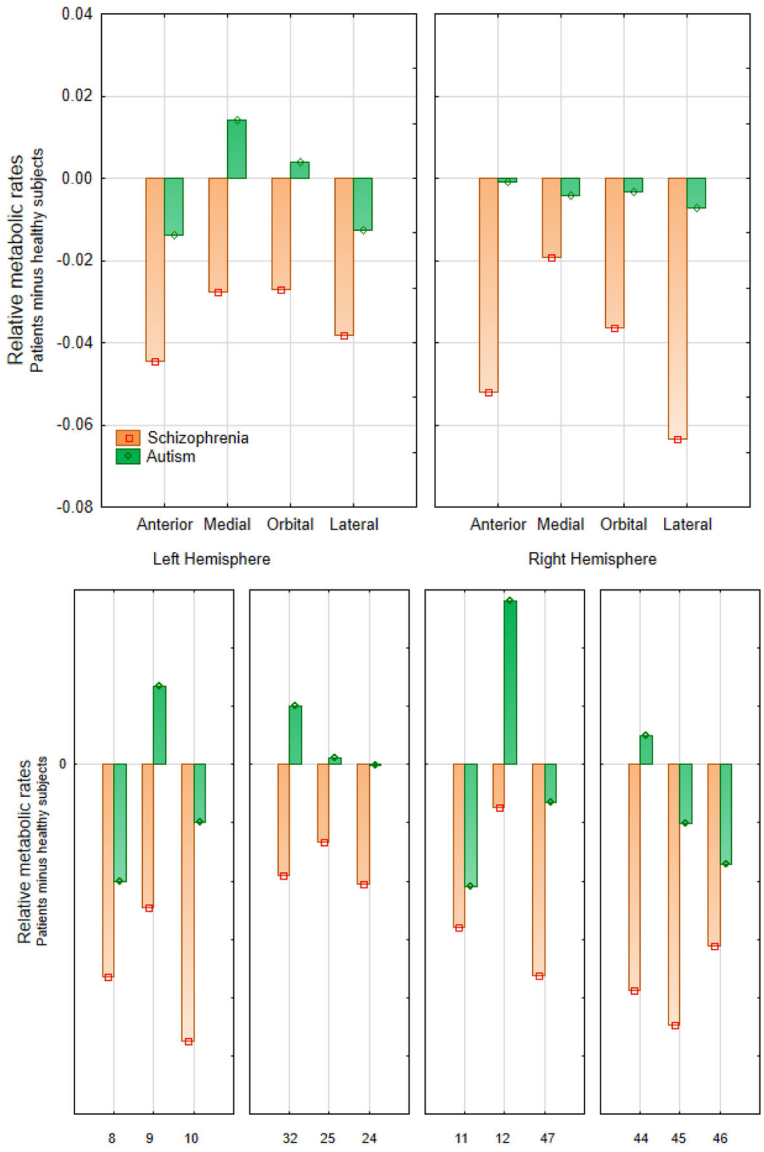

Figure 3.

Three-group ANOVA comparison of ^{18}fluorodeoxyglucose uptake in the prefrontal cortex. Prefrontal cortex was divided into 4 regions, each containing 3 Brodmann areas. The upper panel illustrates the group-by-hemisphere-by-prefrontal region interaction ($F_{6, 354}$=3.74, p=0.001; Wilks' λ =0.87, multivariate $F_{6, 232}$=2.75, p=0.001), the lower panel illustrates the group-by-region-by-Brodmann area interaction ($F_{12, 708}$=1.86, p=0.036; Wilks' λ =0.87, multivariate $F_{2, 117}$=2.75, p=0.033). The Bonferroni testing (p<0.01) confirmed the main effect of diagnostic group. Individual t-tests on the 24 areas (12 in each hemisphere) yielded 14 schizophrenia/healthy control differences at p<0.05 uncorrected; Brodmann areas 10 (left and right), 44 (right), and 45 (right) were significant with the Bonferroni criterion of 0.002.

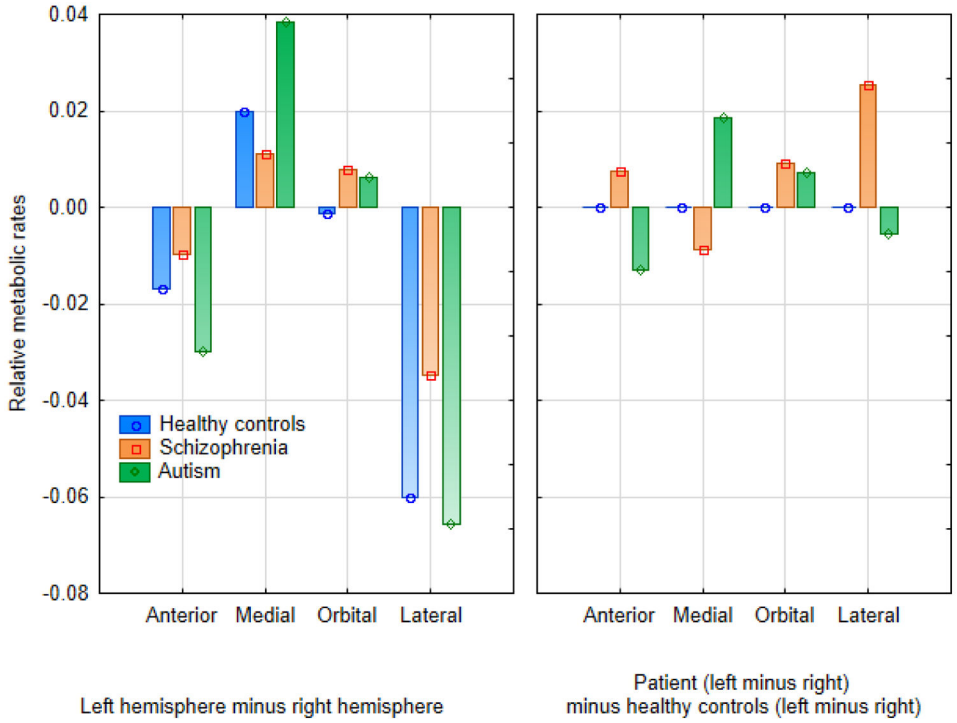

Figure 4.

Hemispheric asymmetry of metabolic rates in the prefrontal cortex.

This figure is based on the significant group-by-hemisphere-by-prefrontal region interaction ($F_{6, 354}$=3.74, p=0.001), confirmed with the Bonferroni correction. The left panel shows the difference in asymmetry in the patient groups compared to healthy controls. The right panel shows the left-minus-right difference in asymmetry in the patient groups (orange and green) compared to healthy controls (zero axis). Bars above zero indicate higher left-minus-right differences in comparison to healthy controls and bars below zero indicate lower left-minus-right differences in comparison to healthy controls.

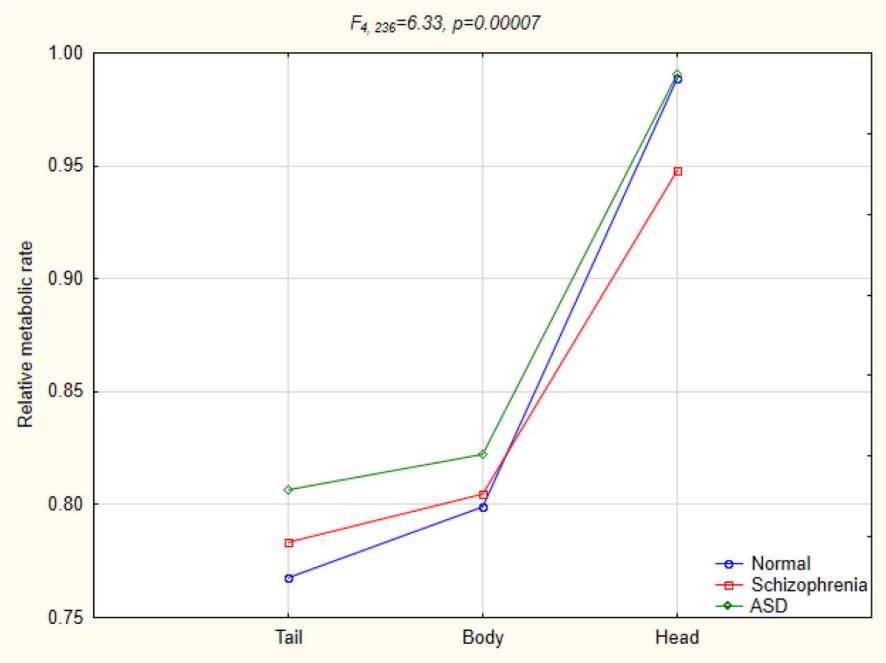

Figure 5.
Three-group ANOVA for the caudate nucleus subregions.

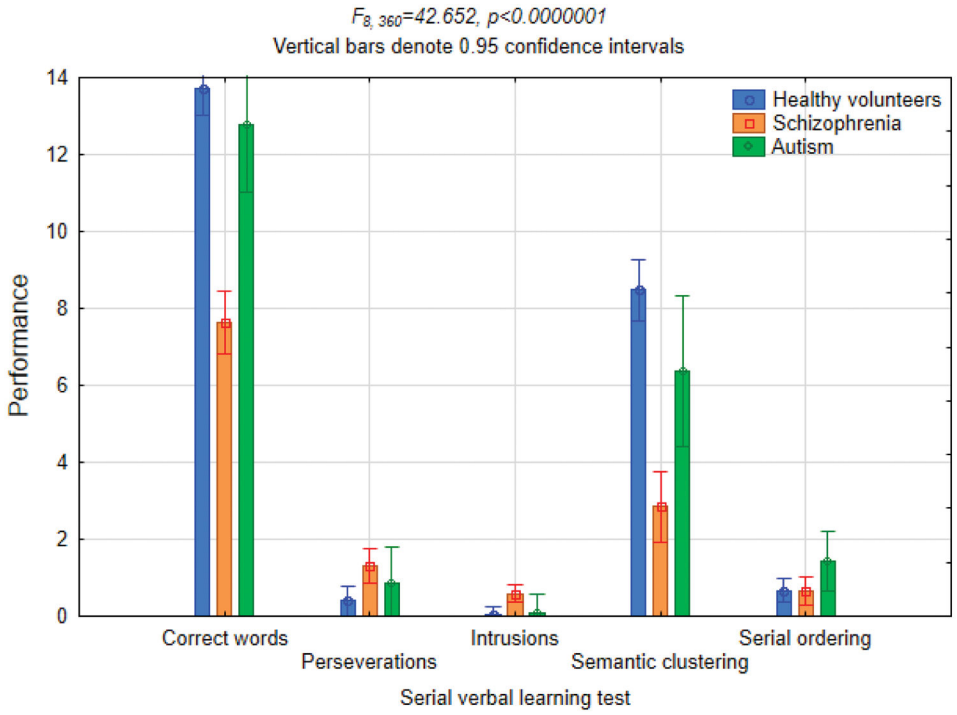

Figure 6.
Three-group ANOVA for the serial verbal learning test performance.

Table 1

Significant ANCOVA interactions for between-group differences in FDG metabolic rates

		ASD vs. schizophrenia vs. normal controls	ASD vs. schizophrenia	ASD vs. normal controls	Schizophrenia vs. normal controls
Whole brain	g×BA	$F_{82, 4797}$=2.20, p<0.0000001 (0.0005)*	*$F_{41, 2583}$=1.57, p<0.01 (0.35)*	$F_{41, 3157}$=2.23, p=0.00001 (0.005)*	$F_{41, 3813}$=2.60, p<0.0000001 (0.01)
Frontal lobe	ME	$F_{2, 117}$=4.91, p=0.009			$F_{1, 93}$=9.88, p=0.002*
	g×BA	$F_{20, 1170}$=2.54, p=0.0002 (0.002)*			$F_{10, 930}$=5.38, p<0.0000001 (0.0036)*
Parietal lobe	ME	$F_{2, 117}$=3.36, p=0.04		$F_{1, 77}$=4.51, p=0.037	
	g×BA	$F_{14, 819}$=3.47, p=0.000002 (0.000005)*	*$F_{7, 441}$=1.99, p=0.055 (0.09)*	$F_{7, 539}$=3.43, p=0.001 (0.000009)*	$F_{7, 651}$=5.70, p=0.000002 (0.00015)*
Occipital lobe	g×BA	*$F_{4, 234}$=2.52, p=0.04 (0.05)*			*$F_{2, 186}$=3.90, p=0.02 (0.09)*
Hippocampus	ME	$F_{2, 117}$=9.71, p=0.0001*		$F_{1, 77}$=13.76, p=0.0004*	$F_{1, 93}$=18.22, p=0.00005*
Hypothalamus	ME	$F_{2, 117}$=4.08, p=0.02	$F_{1, 63}$=7.05, p=0.01		$F_{1, 93}$=6.26, p=0.007
Mammilary bodies			$F_{1, 63}$=4.38, p=0.04		
Thalamic nuclei					
Lateral posterior	ME	$F_{2, 117}$=6.35, p=0.002*	*$F_{1, 63}$=3.84, p=0.055*		$F_{1, 93}$=10.85, p=0.001*
Ventral posteromedial	ME	*$F_{2, 117}$=2.59, p=0.08*			$F_{1, 93}$=5.10, p=0.026
Ventral posterolateral	ME	$F_{2, 117}$=4.34, p=0.015			$F_{1, 93}$=7.93, p=0.006
Pulvinar	ME	$F_{2, 117}$=4.06, p=0.02			$F_{1, 93}$=7.62, p=0.007
Mediodorsal	ME	*$F_{2, 117}$=2.50, p=0.09*			$F_{1, 93}$=4.07, p=0.047
Caudate subdivisions	g×R	$F_{4, 234}$=10.15, p<0.0000001 (0.000035)*		$F_{2, 154}$=6.41, p=0.002 (0.01)	$F_{2, 186}$=18.64, p<0.00000001 (0.000007)*
Head of the caudate	ME	*$F_{2, 117}$=2.64, p=0.08*			$F_{1, 93}$=4.92, p=0.03
Tail of the caudate	ME	$F_{2, 117}$=10.87, p=0.00005*		$F_{1, 77}$=9.69, p=0.003*	$F_{1, 93}$=25.79, p=0.000002*
Putamen	ME	$F_{2, 117}$=6.18, p=0.003*		$F_{1, 77}$=5.76, p=0.02	$F_{1, 93}$=11.62, p=0.001*
Medial globus pallidus	ME	$F_{2, 117}$=4.18, p=0.02		$F_{1, 77}$=7.80, p=0.007	
Lateral globus pallidus	ME	$F_{2, 117}$=4.83, p=0.01		$F_{1, 77}$=8.52, p=0.005	$F_{1, 93}$=4.67, p=0.03
Claustrum	ME	$F_{2, 117}$=10.36, p=0.00007*		$F_{1, 77}$=13.14, p=0.0005*	$F_{1, 93}$=16.86, p=0.00009*
Amygdala	ME	$F_{2, 117}$=4.87, p=0.009		$F_{1, 77}$=7.48, p=0.008	$F_{1, 93}$=8.09, p=0.0055

For all higher-order ANCOVA interactions (i.e. other than the main effects) univariate p-values are followed by multivariate Wilks' λ p-values in parentheses; p-values at trend level of significance (<0.1) are italicized. Abbreviations: ME – main effect of diagnostic group, g×R – group-by-region interaction, g×BA – group-by-Brodmann area interaction.

MANOVA interactions that met the Bonferroni correction are indicated by asterisks. The frontal and parietal lobe group×Brodmann area interactions met the Bonferroni criteria for four brain lobes and two hemispheres (0.05/8=0.00625). We chose all ANOVAs (three diagnostic groups and the 3 paired comparisons by four lobes, 4 x 4=16) as a divisor, but note that this correction could be considered to be

spuriously failing to replicate published findings in schizophrenia and autism literature. For the 16 subcortical regions, at the $p<0.05$ level the three-group main effect was significant for 15 out of 16 tests, the main effect of group for healthy controls vs. schizophrenia comparisons was significant in 14 out of 16 tests, and the main effect of group for healthy controls vs ASD comparisons was significant in 9 out of 16 tests. The Bonferroni correction criterion for 16 subcortical regions was 0.00315 (0.05/16).

Table 2

Changes in metabolic rates in ASD and schizophrenia

ASD and schizophrenia in relation to normal controls	
Greater-than-normal in ASD, lower-than-normal in schizophrenia	Anterior cingulate (areas 32 and 33), frontal area 9 *
	Hypothalamus
Greater-than-normal in schizophrenia, lower-than-normal in ASD	Precentral/postcentral region (areas 2, 3, 4, and 5 *)
Both ASD and schizophrenia are lower-than-normal	Frontal cortex (areas 8 *, 10 *, 11 *, 45 *, 46 *, and 47 *), parietal cortex (39 *, 40 *)
	Amygdala
	Ventral posteromedial nucleus of the thalamus
	Claustrum
Both ASD and schizophrenia are higher-than-normal	Occipital cortex (areas 17 and 18)
	Hippocampus, tail of the caudate
	Pulvinar
	Lateral globus pallidus, medial globus pallidus, putamen
Only ASD is lower-than-normal (no changes in schizophrenia)	Whole parietal lobe **, postcentral areas 1 * and 7 *
Only schizophrenia is lower-than-normal (no changes in ASD)	Whole frontal lobe **
	Head and body of the caudate
	Mediodorsal nucleus of the thalamus
Only schizophrenia is higher-than-normal (no changes in ASD)	Posterior and ventroposterior lateral nuclei of the thalamus
Schizophrenia vs. normal controls	
Schizophrenia is lower-than-normal	Whole frontal lobe **, all frontal areas except area 4
	Parietal area 40, anterior cingulate (24, 25, 32, 33), temporal area 22
	Amygdala
	Head of the caudate
	Mediodorsal and ventral posteromedial nuclei of the thalamus
Schizophrenia is higher-than-normal	Occipital areas 17 and 18
	Hippocampus
	Pulvinar, ventroposterior lateral and lateral posterior nuclei of the thalamus
	Tail of the caudate
	Lateral globus pallidus, putamen, claustrum
ASD vs. normal controls	
ASD is lower-than-normal	Whole parietal lobe **, all parietal areas except area 43
	Frontal areas 6, 8, 11
	Amygdala
ASD is higher-than-normal	Posterior cingulate (23, 29, 30), orbitofrontal (12), occipital areas 17 and 18
	Hippocampus
	Tail of the caudate
	Putamen, medial and lateral globi pallidi, claustrum

* Statistically significant ($p<0.05$) or trend-level ($p<0.1$) interaction in follow-up simple ANCOVA (with age as covariate) with 3 diagnostic groups for individual Brodmann areas (BA, df=2, 117): BA1 F=6.54, p=0.002; BA5 F=3.03, p=0.05; BA7 F=3.44, p=0.035; BA8 F=2.87, p=0.06; BA9

F=2.56, p=0.08; BA10=8.10, p=0.0005; BA11 F=6.35, p=0.002; BA39 F=2.88, p=0.06; BA40 F=6.64, p=0.002; BA44 F=4.31, p=0.02; BA45 F=3.41, p=0.04; BA46 F=3.63, p=0.03; BA47 F=3.44, p=0.035.

** Significant main effect of diagnosis in lobar analyses.